Available online at www.sciencedirect.com
SCIENCE DIRECT®
Precambrian Research 122 (2003) 359–376
Precambrian Research
www.elsevier.com/locate/precamres

Neoproterozoic mafic dike swarms of the Sharyzhalgai metamorphic massif, southern Siberian craton

E.V. Sklyarov [a], D.P. Gladkochub [a], A.M. Mazukabzov [a], Yu.V. Menshagin [a], T. Watanabe [b], S.A. Pisarevsky [c,*]

[a] *Institute of the Earth's Crust, Siberian Branch, Russian Academy of Science, Lermontova Ave. 128, 664033 Irkutsk, Russia*
[b] *Division of Earth and Planetary Sciences, Hokkaido University, Kita 8 Nishi 5, Kita-ku, Sapporo 060-0808, Japan*
[c] *Tectonics Special Research Centre, The University of Western Australia, 35 Stirling Highway, Crawley, WA 6009, Australia*

Received 1 October 2001; received in revised form 29 July 2002; accepted 30 July 2002

Abstract

Geochemical, petrographic, mineralogical and geochronological study of mafic dikes in the Sharyzhalgai massif of the south Siberian craton has revealed the presence of three distinct generations of dikes. The youngest and most abundant dikes are non-metamorphosed and largely unaltered dolerites. They include both tholeiitic and subalkaline types that were probably intruded during a single magmatic episode. A 3-point whole rock-mineral Sm–Nd isochron age of 743 ± 47 Ma indicates that these dikes are Neoproterozoic. The $^{40}Ar/^{39}Ar$ plateau age of 758 ± 4 Ma is broadly in accord with the Sm–Nd age. A geochemical study of these dikes indicates that both tholeiitic and subalkaline dolerites have similar trace element abundances, suggesting that they were derived from a single mantle source. On the basis of their age, it is possible that these dikes were part of either the well-known Franklin swarm in northern Canada, or of the 780 Ma swarm in western Laurentia. However, more evidence is needed to test this hypothesis.

Keywords: Mafic dike swarms; Neoproterozoic; Sharyzhalgai massif; Siberian craton

1. Introduction

Precambrian mafic dikes and sills occur in the metamorphic basement of the Siberian craton and in Meso- to Neoproterozoic sedimentary sequences along the craton margins. Dikes of Meso- to Neoproterozoic age have previously been described in the Anabar shield segment of the craton (Fig. 1A; Ernst et al., 2000) and Neoproterozoic sills occur in a carbonate-terrigenous sequence in the eastern margin of the craton (Rainbird et al., 1998; Frost et al., 1998). Mafic dikes and sills are also abundant along the southwestern margin of the craton (Fig. 1B) but are very poorly described in the literature, mostly in local Russian publications (Domyshev, 1976; Sekerin et al., 1991, 1995; Sklyarov et al., 2000; Gladkotchub et al., 2001). In addition, there are only few robust isotopic ages and rigorous geochemical and mineralogical data for these dike swarms. Taking into account the importance of mafic dikes as indicators of extensional processes in cratons, especially in connection with reconstructions of the supercontinent Rodinia (e.g. Hoffman, 1991; Park et al., 1995; Dalziel, 1997 and references therein), we have studied the dike swarms in the Sharyzhalgai metamorphic massif on the southwestern margin of the Siberian craton, and in this paper we present data

* Corresponding author. Tel.: +61-8-93807844; fax: +61-8-93801090.
E-mail address: spisarev@tsrc.uwa.edu.au (S.A. Pisarevsky).

0301-9268/02/$ – see front matter
PII: S0301-9268(02)00219-X

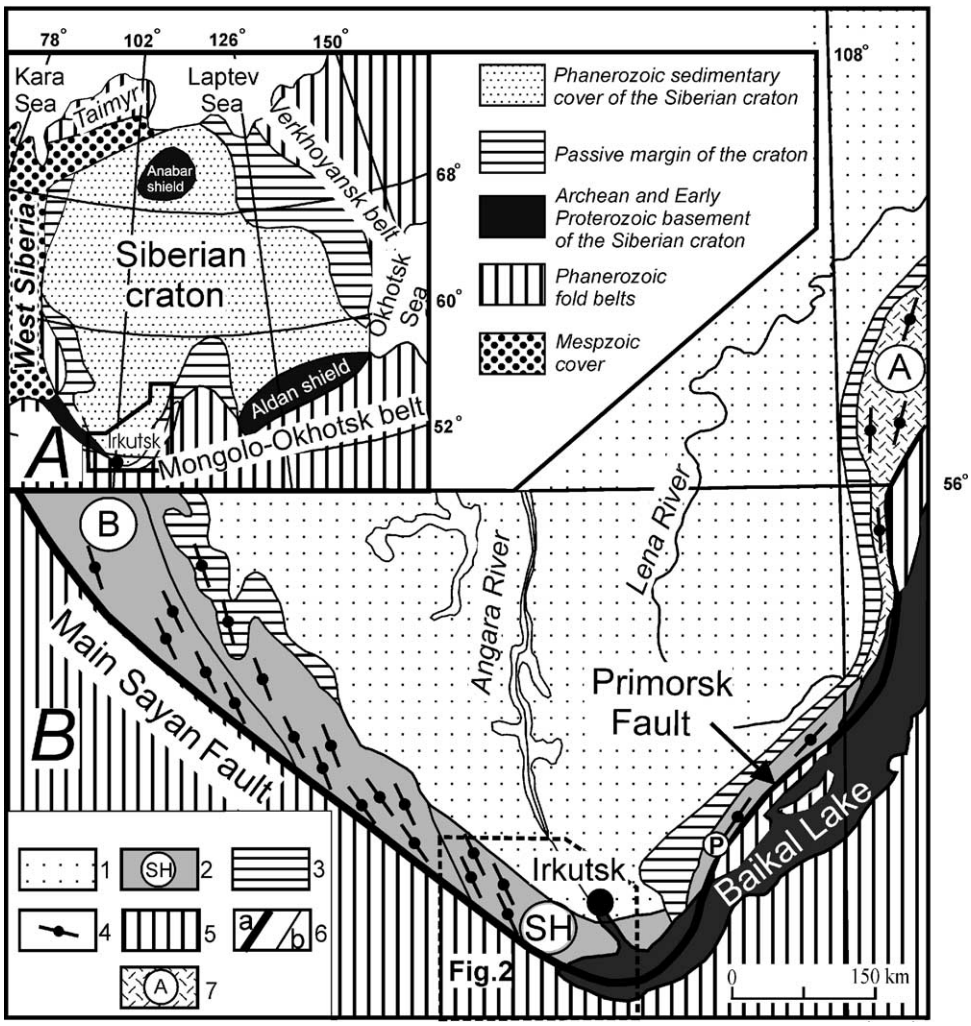

Fig. 1. Tectonic framework of the southern part of the Siberian craton. (1) Phanerozoic sedimentary cover; (2) Archean and Paleoproterozoic metamorphic complexes (B: Biryusa; P: Primirsk; SH: Sharyzhalgai); (3) Meso- to Neoproterozoic passive continental margin succeaaions; (4) Meso- to Neoproterozoic dike swarms; (5) Phanerozoic Sayan-Baikal fold belt; (6a) modern boundary of the Siberian craton based on the geological and geophysical data; (6b) faults; (7) Paleoproterozoic Akitkan volcanic belt.

on the geology, geochemistry and geochronology of the Neoproterozoic mafic dikes.

2. Dike swarms of the southern margin of the Siberian craton

2.1. General geology

The Siberian craton is one of the ancient crustal blocks that make up the Asian continent. Most of the craton is covered by upper Neoproterozoic—lower Paleozoic platform sediments. Metamorphic and magmatic crystalline basement complexes are exposed in the Aldan and Anabar shields and at the southern margin of the craton in several metamorphic massifs (Fig. 1A), e.g. the Sharyzhalgai massif (SH in Fig. 1). The Siberian craton is bounded on its southwestern side by the Main Sayan and Primorsk faults (Fig. 1B).

The southwestern margin of the Siberian craton is structurally and compositionally complex and its

tectonic evolution is still a matter of debate. Phanerozoic platform sediments cover almost the entire region, with Precambrian rock exposures limited to a relatively narrow strip (30–250 km wide) along the cratonic boundary (Fig. 1B). This strip is composed of Archean and Paleoproterozoic metamorphic complexes, the Paleoproterozoic Akitkan volcanic belt, and segments of Meso- to Neoproterozoic passive margin successions (Sklyarov et al., 2000).

These Archean and Paleoproterozoic metamorphic complexes are characterised by granulite- and amphibolite-facies metamorphism and complex, commonly multi-phase deformation. The largest of these massifs, and the subject of this study, the Sharyzhalgai metamorphic massif (Fig. 2), is composed of granitic gneiss and granulite-facies metamorphic terranes intruded by Paleoproterozoic granites (e.g. Sklyarov et al., 2001). The massif underwent two stages of high-grade metamorphism (Aftalion et al., 1991; Sklyarov et al., 1998). The early, high-P granulite-facies metamorphism (T = 700–900 °C, P = 9–14 kbar) has been interpreted to reflect the main Paleoproterozoic collisional event that led to amalgamation of late Archean and early Paleoproterozoic terranes (Aftalion et al., 1991), whereas the later low-P metamorphism (T = 700–850 °C, P = 4–6 kbar) has been linked to the collapse of the Paleoproterozoic orogen. Localised younger reworking and retrogression at low-temperature (greenschist and low amphibolite-facies) occurred in narrow shear zones.

The Paleoproterozoic Akitkan volcanic belt (Fig. 1B) stretches from the northern shore of Lake Baikal across the Siberian craton for a distance of about 2000 km (Condie and Rosen, 1994). The belt is composed of volcanic rocks, mainly felsic in composition with minor mafic components (Bukharov, 1987; Neimark et al., 1998), associated with red-coloured lacustrine and shallow-water marine sediments, including conglomerate, gritstone, sandstone, siltstone and tuffaceous rocks. The granitoids of the Primorsk Complex (Fig. 1B), including rapakivi varieties, are regarded as the intrusive equivalents of the volcanic rocks. U–Pb (zircon) ages of the volcanic rocks and

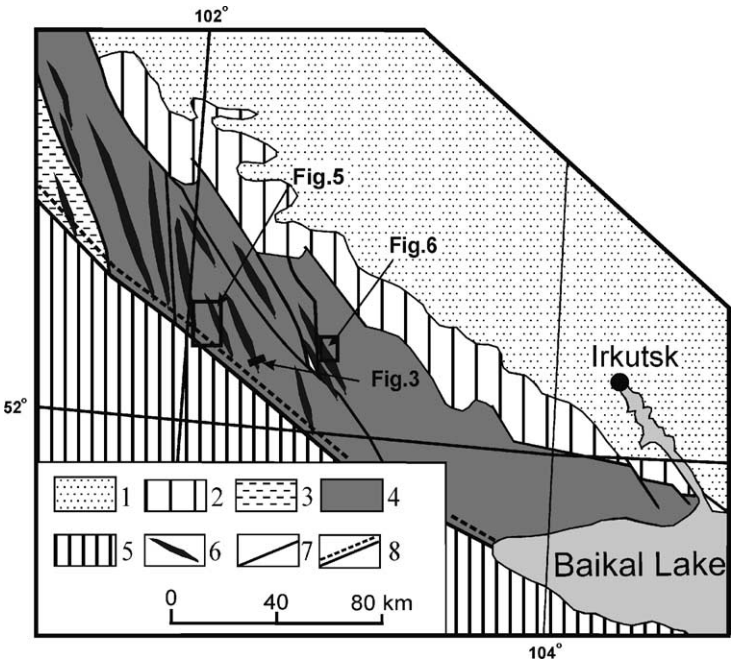

Fig. 2. Tectonic map of the Sharyzhalgai metamorphic massif. (1) Phanerozoic sedimentary cover of the Siberian platform; (2) Mesozoic depressions; (3) Neoproterozoic volcanic and sedimentary rocks; (4) Sharyzhalgai metamorphic massif; (5) Phanerozoic Sayan-Baikal fold belt; (6) Neoproterozoic dike swarms; (7) faults; (8) Main Sayan fault (suture separating craton and fold belt).

co-genetic granites range between 1880 and 1860 Ma (Neimark et al., 1998).

Remnants of the Meso- to Neoproterozoic passive continental margin of the southern Siberian craton (Fig. 1B) are structurally complex and are mostly composed of thick sedimentary and volcanic sequences, with locally exposed small fragments of the Paleoproterozoic metamorphic basement. Grade of metamorphism in the volcanic and sedimentary sequences generally does not exceed greenschist facies.

2.2. Mafic dikes

Precambrian dike swarms, locally associated with sill complexes, occur along the Siberian craton boundary including the Sharyzhalgai metamorphic massif (Figs. 1B and 2). Mapped lengths of individual dikes range up to 3–8 km, with their thicknesses varying from 1–2 m up to 50 m. The compositions of most dikes in the Akitkan belt (Fig. 1B) correspond to subalkaline basalts, but vary from low-K tholeiite through subalkaline basalt to alkaline basalt in terranes south of the Akitkan belt, including the Sharyzhalgai massif (Fig. 1B).

Geological constraints suggest that the ages of these dikes range between 1860 and 650 Ma. They are older than Vendian (~650–550 Ma), as they do not cut Vendian sediments. Their maximum age is uncertain due to the paucity of reliable isotopic data, variable overprinting events during later metamorphism and deformation, and unknown relationships between different generations of dikes. The dikes cut rocks of the Akitkan volcanic belt, which have well constrained U–Pb (zircon) ages of between 1800 and 1860 Ma (Neimark et al., 1998), and are overlain by Neoproterozoic sedimentary sequences (Khomentovsky, 1996). Some of the dikes cut Paleoproterozoic metamorphic and magmatic complexes and Mesoproterozoic sedimentary and volcanic sequences, and are inferred to be between 1200 and 800 Ma (Sryvtsev, 1986). A few K–Ar and Rb–Sr dates (Domyshev, 1976; Sekerin et al., 1991, 1995) suggest that the dikes may be subdivided into two groups with ages of 1650–1550 Ma and 1200–800 Ma.

Previous attempts to separate different generations of dikes (Sekerin et al., 1995; Sklyarov et al., 2000) were based mostly on geological data. However, the relationships between these generations are unclear due to a lack of precise ages and to an absence of exposed cross-cutting relationships.

3. Dike swarms in the Sharyzhalgai metamorphic massif

3.1. Three generations of dikes

Mafic dikes are abundant in several areas of the Sharyzhalgai metamorphic massif (Fig. 2). Most dikes have NNW to NW trends and are nearly vertical. However, a few shallowly-dipping dikes occur in some localities. Thicknesses of dikes range from 20–30 cm to 3–5 m (occasionally up to 30 m), and some dikes in well-exposed areas can be traced for distances of 1–10 km. Examples of the distribution of dikes and their field relationships are shown for representative areas (Figs. 3–6).

The majority of dikes in the Sharyzhalgai metamorphic massif is relatively fresh. Domyshev (1976) suggested that they all are part of a single swarm he termed the Nersinsk complex. However, we have found two subsets of older, metamorphosed dikes, implying at least three episodes of dike emplacement.

The main criteria used for the discrimination of generations of mafic dikes are their grade of metamorphism and the geological relations between dikes. Dikes and small stocks of the first generation are composed of fine- to medium-grained garnet amphibolite and garnet-bearing mafic granulite. They were metamorphosed under high-*P* granulite- to amphibolite-facies conditions. Dikes of the second generation are characterised by garnet-free, two pyroxene–biotite–plagioclase assemblages, indicating that they were metamorphosed under low-*P* granulite-facies conditions. These second generation dikes are much less abundant than the older and younger ones. Dikes of the third generation are represented by non-metamorphosed dolerite and gabbro-dolerite, although a few of these dikes underwent minor low-temperature alteration (observed only in shear zones of Paleozoic or younger age).

The first generation dikes and sills are commonly nearly conformable to the foliation of the host rocks and occur as planar bodies (Fig. 3), which are typically 5–10 m thick, locally up to 100–200 m thick. Individual dikes can be traced for distances of 100 m to

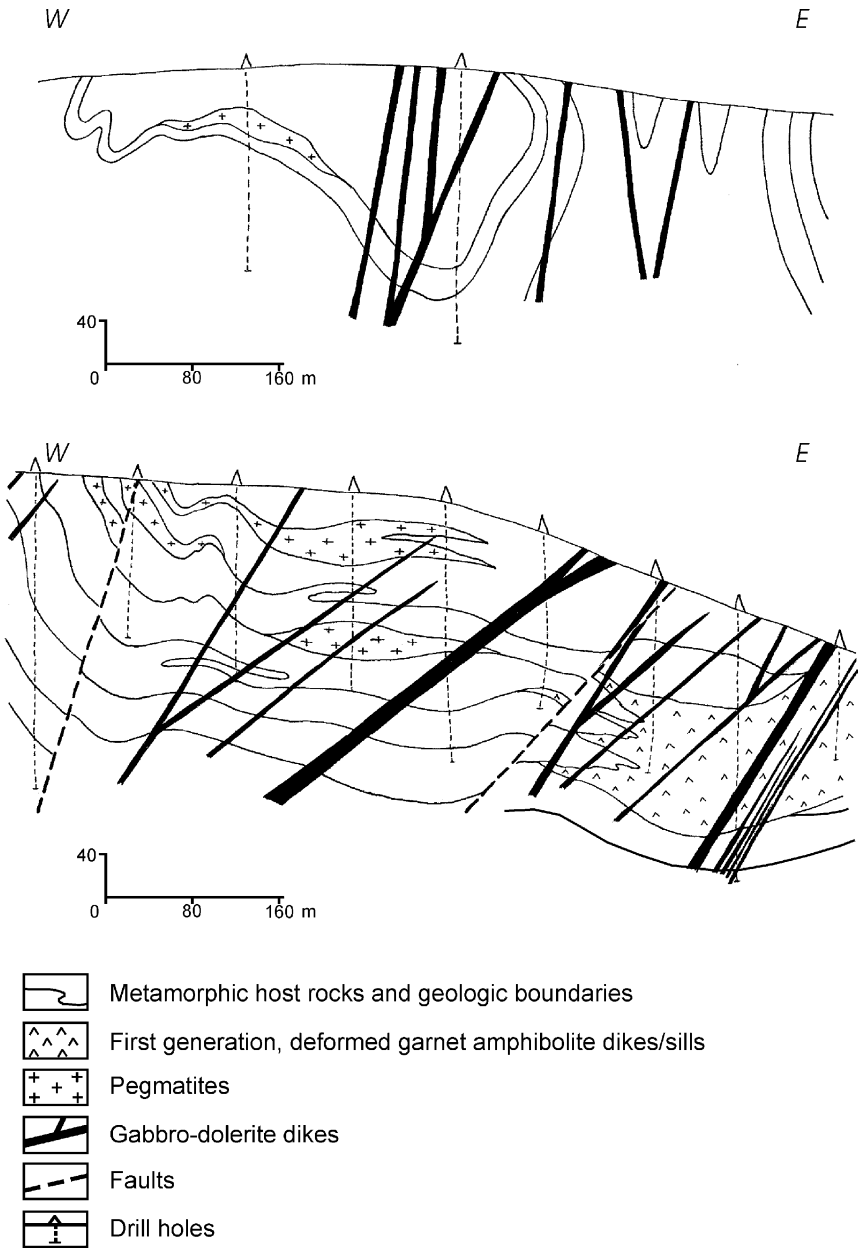

Fig. 3. Cross-cutting relationships between the first and third generation dikes. Geological cross-sections of the sillimanite ore deposit on the left bank of the Kitoy River, compiled from detailed geological mapping and drill core data.

1 km. However, in other cases these dikes are discordant to the foliation of country rocks and are deformed and boudinaged. No remnants of magmatic texture are preserved in these dikes. Relations between these and younger dikes have been observed in few places only, for example, in the area of the Kitoy sillimanite deposit (Fig. 3).

Dikes of the second generation are rare and have been documented in only a few localities. Some relics of their magmatic textures are locally preserved.

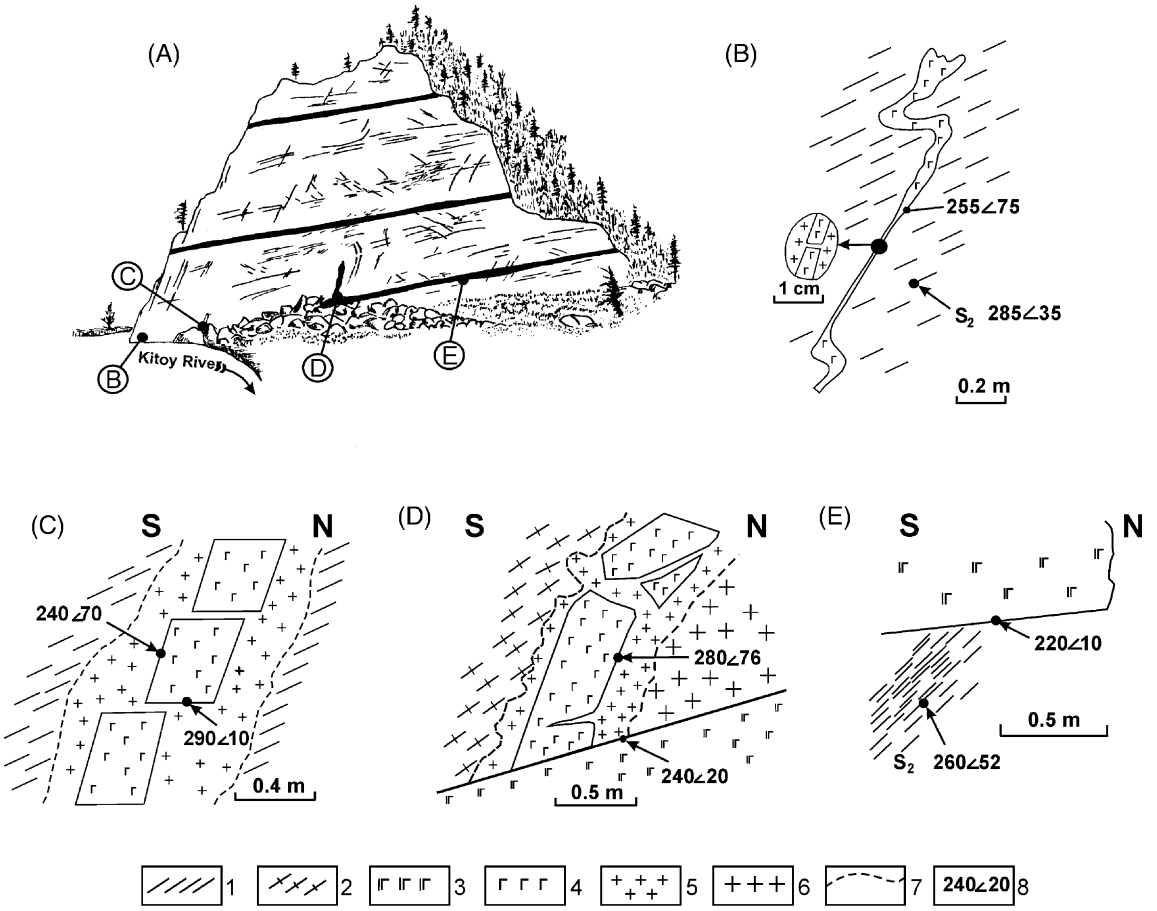

Fig. 4. Cross-cutting relationships between the second and third generation dikes. Field sketches at the Proval locality (Kitoy River). (1) Migmatized gneiss; (2) granite-gneiss; (3) Neoproterozoic dolerite (third generation dike); (4) second generation dike; (5) fine-grained granite along dikes; (6) late Archean granite; (7) contact between newly formed granite and host gneiss and granite; (8) dip of foliation in gneiss and dip of dikes. (A) Sketch of cliff with exposed dikes, thin boudinaged relics of second generation dikes, and a set of gently dipping Neoproterozoic gabbro-dolerite (third generation dikes). (B) Thin, deformed second generation dike in granite-gneiss. (C) Boudinaged second generation dike, enclosed in fine-grained granite near the dike. (D) Cross-cutting relationship between dikes of the second and third generations. (E) Contact of the gently dipping third generation dike with host granite-gneiss.

Field relationships between these dikes and non-metamorphosed dolerite (third generation dikes) have been documented at Proval on the left bank of the Kitoy River (Fig. 4). There, steep thin dikes of the second generation cut Archean granite-gneiss and coarse-grained Archean granite (Fig. 4B–D). The dike contact zones are marked by fine-grained granite. Some dikes are boudinaged and cut by the granite, implying that the dike magma was deformed before it cooled (Fig. 4B–D). No such granites are found at the contact zones of third generation dikes (Fig. 4D and E).

Most of the dikes in the Sharyzhalgai metamorphic massif belong to the third generation. These dikes are typically 1.5–3 m thick and consist of unaltered dolerite, locally with minor low-grade metamorphic alteration (chlorite after pyroxene, calcite after plagioclase). Chilled margins are common. In most areas, the dikes dip steeply and have a consistent NW-SE trend. For example, dikes in the Onot River basin (Fig. 5)

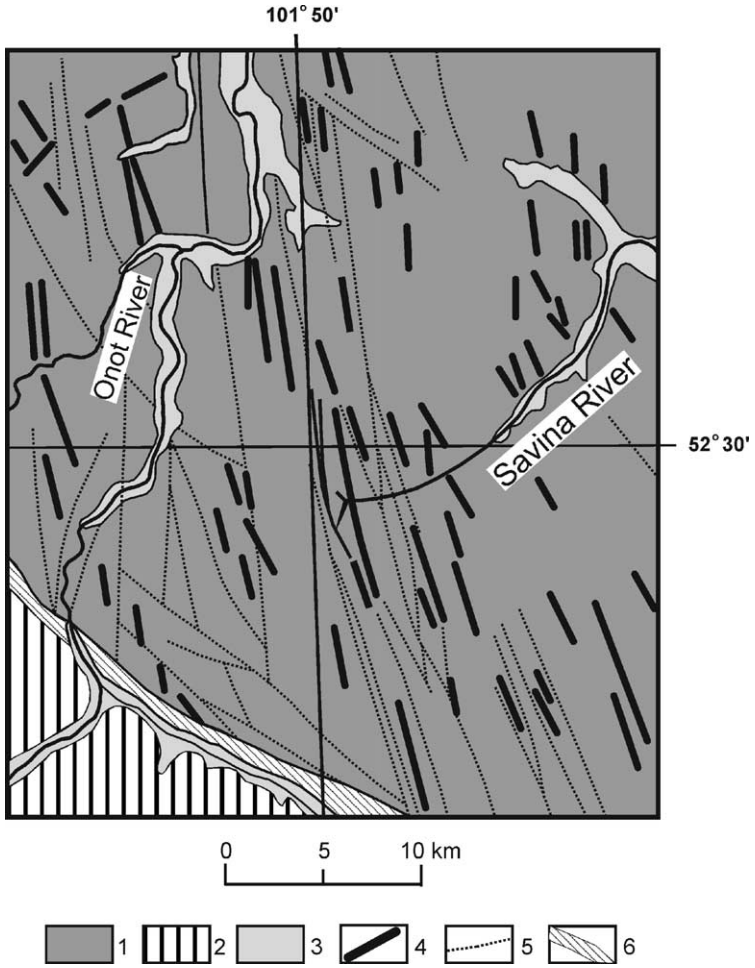

Fig. 5. Geological map of the Onot area of the Sharyzhalgai metamorphic massif. (1) Archean–Paleoproterozoic metamorphic complex (undifferentiated); (2) metamorphic complexes of the Sayan-Baikal fold belt; (3) Cenozoic sediments; (4) third generation dikes; (5) main faults; (6) Main Sayan fault.

strike N-NW, oblique to the main suture separating the Siberian craton from the Paleozoic fold belt. Some of the dikes can be traced up to 7–8 km, but individual bodies may reach 12–15 km in length according to aeromagnetic data. Locally these dikes are subhorizontal and roughly parallel to the foliation of the host granite-gneiss (Fig. 4A and E, Fig. 6). They cut the second generation metamorphosed dikes (Fig. 4D).

Aftalion et al. (1991) determined the age of the main collisional metamorphic event in this area to be between 2000 and 1900 Ma. First generation dikes were metamorphosed under high-*P* high-*T* conditions, which was inferred to have taken place at this time. Thus, the first generation dikes in the Sharyzhalgai metamorphic massif should be older than 2000–1900 Ma. Dikes of the second generation were intruded during a subsequent low-*P* high-*T* metamorphism, probably caused by the collapse of Paleoproterozoic orogen and subsequent extension at 1890–1860 Ma (Aftalion et al., 1991). The time of emplacement of the most abundant dikes of the third generation is loosely constrained between 1860 and 650 Ma. The results of geochemical and isotopic studies of these youngest dikes are described below.

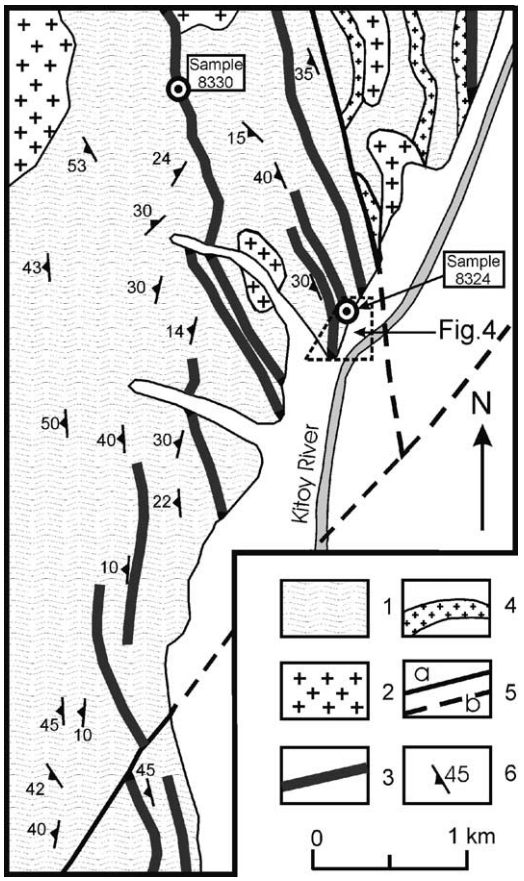

Fig. 6. Neoproterozoic dikes of the Kitoy River area. (1) Archean and Paleoproterozoic gneiss and granite-gneiss (undifferentiated); (2) Paleoproterozoic granite; (3) Neoproterozoic gabbro-dolerite; (4) marble; (5) faults, exposed (a) and inferred under Cenozoic cover (b); (6) strike and dip of the foliation.

3.2. Petrography and mineralogy of the third generation dikes

Most of these rocks are well-crystallised dolerite and gabbro-dolerite with ophitic and poikilitic-ophitic textures. The main rock-forming minerals are clinopyroxene and plagioclase in variable proportions; Ti-magnetite is the typical accessory oxide mineral. Olivine, pigeonite, and chrome spinel (as inclusions in olivine) are present only in some high-Mg dolerite dikes. All minerals were analysed using a modified MAR-3 microprobe in the Geological Institute SB RAS (Ulan-Ude) using standard conditions of analysis (operators Karmanov and Kanakin). Fifty analyses were performed on six samples. Representative results are listed in Table 1.

Plagioclase is idiomorphic, forming elongate prismatic or lath-like crystals, having both albite and Carlsbad twinning. It is usually fresh, and only locally partly to completely replaced by fine-grained aggregates of epidote–muscovite–chlorite. Plagioclase compositions vary between dikes, but are mostly andesine-labradorite (An_{30}–An_{70}). Zonation is usual, with the An component decreasing by 10–15% at the rims. No significant compositional differences are seen between large idiomorphic crystals and small laths in the matrix, and the most calcic plagioclase occurs in olivine-bearing dolerite.

Clinopyroxene (subcalcic augite, subcalcic salite, and rarely pigeonite) usually forms near isometric, prismatic or irregular crystals. Sharp compositional changes occur even in single grains (see Table 1), possibly due to intergrowth of different pyroxene phases. Occurrence of low-Ca clinopyroxene in the absence of orthopyroxene suggests rapid crystallisation during fast cooling of the melt. The main trends of clinopyroxene composition from core to rim are a decrease of Ca and an increase of Fe/Mg ratio.

Olivine forms small (<0.1 mm) subidiomorphic to idiomorphic grains, usually with networks of fractures in high-Mg samples. Grains are usually fresh, with rims only partly replaced by serpentine–talc–carbonate aggregates. Fe/Mg ratios vary by 15–25% and are similar or slightly lower than those of associated pyroxene.

Irregular grains of Ti-magnetite may comprise one modal percent. Cr-spinel occurs only as inclusions in olivine in high-magnesium samples, as rounded isometric grains <0.01 mm. Their compositions (Table 1) are typical of mafic systems except for their relatively high Al_2O_3 contents. Cr-spinels of similar composition have been reported from gabbro-dolerite in the Karoo province and the Siberian platform traps (Plaksenko, 1989).

3.3. Whole rock geochemistry of the dikes of the third generation

Over 80 samples from different localities were selected for whole rock geochemical study, mostly from the Onot (Fig. 5) and Kitoy (Fig. 6) areas. All analysed samples show only minor secondary alteration. Major

Table 1
Representative chemical composition of major minerals from the third generation gabbro-dolerites of the Sharyzhalgai massif

Component	8916							Ti-mgt	81602				
	Ol_c	Ol_r	Cpx	Opx	Pl_c	Pl_r	Ch-sp_{inc}		Cpx	Opx	Pl_c	Pl_r	Mgt
SiO_2	39.52	39.22	51.81	52.23	49.29	55.52	0.00	0.00	51.54	51.94	55.91	51.70	0.53
TiO_2	0.13	0.00	0.30	0.32	0.00	0.00	0.27	19.67	0.39	0.18	0.00	0.00	0.14
Al_2O_3	0.00	0.00	3.66	1.77	31.95	27.86	25.60	2.48	3.88	0.68	28.26	30.39	0.00
Cr_2O_3	0.11	0.11	0.64	0.07	0.00	0.00	36.55	0.15	0.08	0.00	0.00	0.00	0.09
Fe_2O_3	0.00	0.00	0.14	0.89	0.00	0.00	7.97	26.44	0.36	0.07	0.00	0.00	67.33
FeO	15.81	18.97	7.30	14.75	0.51	0.88	16.91	48.74	12.47	25.12	0.20	0.23	31.50
MnO	0.24	0.20	0.20	0.40	0.00	0.00	0.51	0.15	0.24	0.59	0.00	0.00	0.11
MgO	43.82	41.26	17.24	20.41	0.35	0.14	12.33	0.11	16.88	20.06	0.00	0.00	0.14
CaO	0.29	0.20	17.87	8.27	15.13	10.10	0.00	0.00	12.59	0.63	12.73	10.76	0.00
Na_2O	0.00	0.00	0.24	0.13	2.84	5.26	0.00	0.00	0.53	0.00	5.57	4.13	0.00
K_2O	0.00	0.00	0.00	0.00	0.12	0.56	0.00	0.00	0.19	0.00	0.19	0.04	0.00
Total	99.91	99.96	99.40	99.25	100.18	100.32	100.14	97.74	99.15	99.27	100.89	99.22	99.84
Si	0.998	1.004	1.909	1.943	2.253	2.502	0.000	0.000	1.922	1.978	2.499	2.363	0.020
Ti	0.002	0.000	0.008	0.009	0.000	0.000	0.006	0.563	0.011	0.005	0.000	0.000	0.004
Al	0.000	0.000	0.159	0.078	1.721	1.480	0.922	0.111	0.170	0.031	1.489	1.638	0.000
Cr	0.002	0.002	0.019	0.002	0.000	0.000	0.883	0.004	0.002	0.000	0.000	0.000	0.003
Fe^{3+}	0.000	0.000	0.004	0.025	0.000	0.000	0.183	0.758	0.010	0.002	0.000	0.000	1.948
Fe^{2+}	0.334	0.406	0.225	0.459	0.019	0.033	0.432	1.553	0.389	0.800	0.007	0.009	1.013
Mn	0.005	0.004	0.006	0.013	0.000	0.000	0.013	0.005	0.008	0.019	0.000	0.000	0.004
Mg	1.649	1.574	0.947	1.132	0.024	0.010	0.561	0.006	0.938	1.139	0.000	0.000	0.008
Ca	0.008	0.005	0.706	0.330	0.741	0.488	0.000	0.000	0.503	0.026	0.515	0.624	0.000
Na	0.000	0.000	0.017	0.010	0.251	0.460	0.000	0.000	0.038	0.000	0.483	0.366	0.000
K	0.000	0.000	0.000	0.000	0.007	0.032	0.000	0.000	0.009	0.000	0.011	0.002	0.000
Total	2.999	2.995	4.000	4.000	5.016	5.005	3.000	3.000	4.000	4.000	5.004	5.002	3.000

Notes: Ol: olivine; Cpx: clinopyroxene; Opx: orthopyroxene; Pl: plagioclase; Ch-sp: chrome-spinel; Ti-mgt: titanomagnetite; Mgt: magnenite; c: grain core; r: outer rim; inc: inclusion in olivine. Fe^{2+} and Fe^{3+} were estimated by method of Droop (1987).

elements were determined by wet chemical analysis at the Institute of the Earth's Crust (SB RAS), and abundances of Cr, Ni, Co and V were determined by X-ray fluorescence (XRF) at the same institute. Other trace elements and rare earth elements (REE) were determined by inductively coupled plasma-mass spectrometry (ICP-MS) using a VG Plasmaquad PQ-2 Plus (VG Elemental) in the Limnological Institute (SB RAS). Instrumental configuration and operating conditions are given by Garbe-Schonberg (1993), who also describes the acid dissolution technique used to prepare the samples. Because of the possibility of element mobilisation during late alteration, we place emphasis on elements that are relatively immobile during metamorphism (Zr, Nb, Y, Ti, and REE) in our interpretations. Major, trace element and REE analyses for dolerites from the Neoproterozoic dike swarms are presented in Table 2.

Chemically, all the analysed dolerites and gabbro-dolerites are basalts. On an alkali-SiO_2 diagram (Le Bas et al., 1986) the samples straddle the boundary between alkaline and tholeiitic basalts, with most falling in the tholeiitic field (Fig. 7). Because Ti, Zr, Nb, Y are virtually immobile during alteration, whereas Na and K are not, the Zr/TiO2–Nb/Y diagram of Winchester and Floyd (1976) is more reliable for distinguishing rock types than the alkali-based scheme. On this diagram the dikes clearly fall in the basaltic field (Fig. 8). The majority of them plots within the tholeiitic basalt field, with a small subset plotting well within the subalkali basalt field.

3.3.1. Trace element compositions and chemical variations

The studied dikes show a wide compositional range, from most primitive tholeiites (e.g. sample 8326), with

Table 2
Representative compositions of the Neoproterozoic gabbro-dolerites of the Sharyzhalgai massif

Component	8330 (1)	8924 (2)	8326 (3)	81609 (4)	8324 (5)	7004 (6)	8918 (7)	8920 (8)	8925 (9)	81606 (10)	81608 (11)
SiO_2	47.31	49.75	46.03	45.10	48.34	50.14	49.52	49.91	54.66	51.82	48.67
TiO_2	0.4	0.94	0.34	0.75	0.55	0.67	1.06	1.39	1.54	1.18	0.75
Al_2O_3	13.5	14.23	11.95	15.43	13.35	13.03	14.05	13.85	13.70	13.92	15.95
Fe_2O_3	1.82	0.99	1.43	2.52	1.15	3.30	2.07	2.57	3.46	2.14	1.50
FeO	8.63	10.64	9.22	8.15	9.17	12.80	11.08	10.36	11.37	7.46	9.67
MnO	0.18	0.21	0.18	0.14	0.18	0.20	0.18	0.16	0.22	0.15	0.17
MgO	13.31	8.15	18.25	6.77	12.4	6.06	7.23	6.88	3.21	7.62	7.58
CaO	10.09	12.58	8.69	10.97	9.43	10.10	11.15	10.95	8.43	9.03	10.30
Na_2O	1.55	1.84	1.35	1.60	1.65	1.22	2.00	2.50	2.14	2.74	1.94
K_2O	0.22	0.19	0.15	0.69	0.4	0.73	0.28	0.38	0.64	0.91	0.54
P_2O_5	0.06	0.06	0.05	0.06	0.07	0.14	0.06	0.08	0.07	0.71	0.08
H_2O	0.1	0.20	0.06	0.28	0.18	0.40	0.30	0.03	0.03	0.13	0.13
LOI	2.44	0.70	1.81	7.13	2.78	1.20	1.40	1.50	0.96	1.78	2.61
Total	99.61	100.48	99.51	99.59	99.65	99.99	100.38	100.56	100.43	99.59	99.89
U	0.04	0.14	0.05	0.08	0.08	0.15	0.11	0.13	0.45	0.19	0.09
Th	0.56	0.62	0.4	0.38	0.43	0.89	0.36	0.52	1.15	0.27	0.29
Zr	30	24	24	44	40	47	21	72	100	35	42
Hf	0.85	0.79	0.74	1.14	1.19	1.32	0.75	0.57	1.14	1.01	1.28
Ta	0.13	0.14	0.08	0.39	0.49	1.69	0.26	4.10	5.06	0.13	0.19
Nb	1.16	1.84	0.93	4.86	2.27	3.71	2.55	5.38	5.16	1.82	4.35
Y	13.70	18.10	14.98	15.39	17.33	22.43	15.30	22.26	20.45	16.20	16.80
Pb	0.77	1.05	1.09	4.77	1.52	3.43	3.46	2.65	2.87	2.42	2.38
Sc	35.11	38.20	33.13	33.16	39.11	44.03	23.20	39.53	26.21	34.00	19.60
V	140	260	200	250	240	210	390	410	500	220	198
Cr	940	210	880	220	690	183	110	110	28	180	90
Ni	460	110	750	130	330	92	94	91	31	114	85
Co	58	63	78	51	69	70	75	65	59	54	42
Rb	13.52	4.16	3.49	22.63	11.30	25.45	0.81	8.60	10.84	14.11	2.64
Sr	82	101	41	171	120	133	207	327	100	99	175
Ba	105	35	56	223	190	240	47	44	200	146	245
La	4.82	3.45	3.59	4.86	5.59	6.45	4.45	4.97	12.65	14.00	7.08
Ce	10.11	8.53	7.96	11.22	12.4	15.84	10.80	12.80	27.75	21.40	14.80
Pr	1.21	1.24	1.15	1.63	1.5	2.38	1.60	2.10	3.44	2.67	1.89
Nd	4.95	6.00	3.92	7.17	6.28	9.93	7.72	9.06	13.48	8.49	8.10
Sm	1.33	1.94	0.94	1.71	1.6	2.07	2.38	2.64	2.94	1.60	1.89
Eu	0.40	0.73	0.35	0.72	0.62	0.70	0.87	1.13	1.02	0.61	0.79
Gd	1.66	2.55	1.35	2.07	1.98	2.48	2.50	3.22	3.25	2.17	2.39
Tb	0.36	0.47	0.27	0.36	0.39	0.44	0.47	0.57	0.53	0.41	0.44
Dy	2.39	2.99	1.81	2.31	2.51	2.97	2.85	3.40	0.06	2.76	2.85
Ho	0.53	0.66	0.47	0.54	0.62	0.76	0.63	0.76	0.66	0.62	0.67
Er	1.74	1.90	1.38	1.62	1.9	2.40	1.69	2.21	1.87	1.82	1.98
Tm	0.27	0.31	0.25	0.28	0.36	0.48	0.28	0.39	0.32	0.31	0.32
Yb	1.68	1.84	1.80	1.87	2.32	3.27	1.74	2.50	2.09	1.84	2.02
Lu	0.25	0.24	0.25	0.29	0.34	0.28	0.24	0.34	0.30	0.28	0.29

Notes: 1–7: tholeiites; 8–11: subalkaline gabbro-dolerites. Major elements are in wt.%, trace, REE are in ppm.

Mg# 77, Ni 750 ppm, Cr 880 ppm (where Mg# = 100 $Mg^{2+}/(Mg^{2+} + Fe^{2+})$), to highly fractionated subalkaline and alkaline basalts (e.g. sample 8925), with Mg# 36, Ni 31 ppm, Cr 28 ppm (Table 2, Fig. 9). The majority of samples appear to form a single tholeiite—subalkaline group. Several samples appear to represent a primary mantle-derived magma (Mg# > 70), but most dikes are fractionated, which is important for the discussion of mantle sources. Comparison of trace element variations allows recognition of the role of

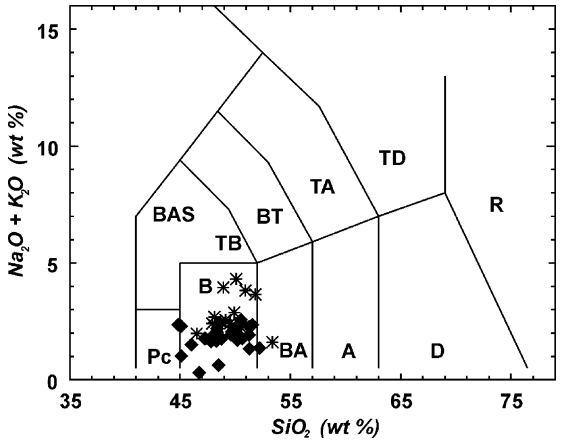

Fig. 7. Classification of dolerites, using the total alkali-SiO_2 diagram of Le Bas et al. (1986). Symbols: filled diamonds: tholeiitic dolerite; asterisks: subalkaline dolerite. A: andesite; B: basalt; BA: basaltic andesite; BAS: basanite; BT: basaltic trachyandesite; D: dacite; Pc: picrobasalt; R: rhyolite; TA: trachyandesite; TB: trachybasalt; TD: trachydacite.

crystal fractionation. For example, concentrations of Ni and Cr systematically decrease as Mg# decreases (Fig. 9A and B), suggesting fractionation of olivine and chromite, or olivine and clinopyroxene from an originally more mafic magma. A small negative Sr anomaly in one sample (Fig. 10) indicates possible plagioclase fractionation. There are clear correlations between Mg# and abundances of TiO_2, Zr, Nb and Y (Fig. 9C–F). Concentrations of all these elements increase with decreasing Mg#, showing that Zr, Nb, Y and Ti remained incompatible with crystallizing assemblages throughout the tholeiitic to subalkaline series.

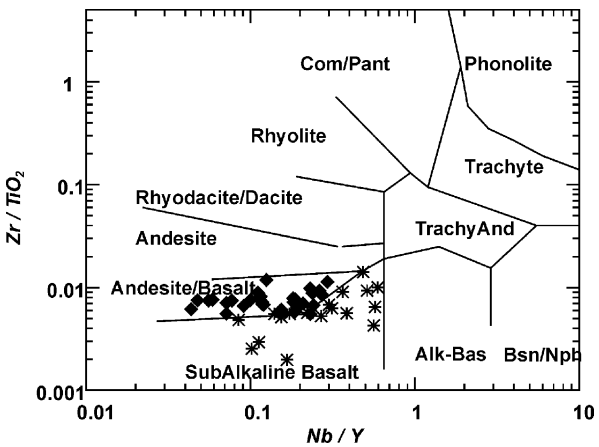

Fig. 8. Zr–TiO_2–Nb/Y diagram (Winchester and Floyd, 1976) for classification of dolerites. Symbols as in Fig. 7.

Ternary proportions of Zr, Nb, Y (Meschede, 1986) (Fig. 11) in tholeiites from the dike swarms are similar to those of normal mid-ocean ridge basalt (N-MORB). Subalkaline dikes generally correspond to the N-MORB and enriched-MORB (E-MORB) and partly to the within plate basalt (WPB) fields, which includes continental flood basalts, continental-rift basalts, and oceanic island basalts. Alkaline basalts, which are enriched in incompatible elements, also plot within the WPB field (Fig. 11). A Zr versus Zr/Y diagram (Pearce and Norry, 1979) (Fig. 12) gives further support for distinguishing two distinct types of dikes, i.e. MORB (tholeiitic) and WPB (alkaline) types. Tholeiitic dikes generally fall in the MORB-field and transitional positions are occupied by subalkaline basalts, which fall in the MORB and WPB fields (Fig. 12).

Both tholeiitic and subalkaline series samples show significant negative *P* anomalies in spider diagrams (Fig. 10), which could reflect fractionation of apatite.

3.3.2. Rare earth elements

Chondrite-normalised (Sun and McDonough, 1989) REE abundances for representative dolerites of all types are plotted in Fig. 13. Analysed tholeiitic and subalkaline dolerites have subparallel REE trends, exhibiting slightly LREE-enrichment and flat MREE and HREE patterns. La_N/Yb_N enrichment factors vary from 1.34 to 2.96 in the tholeiites, and from 1.43 to 5.66 in the subalkaline dolerites. In general, REE abundances in tholeiitic dikes are low and comparable with typical N-MORB. However, several tholeiitic dolerites in the studied area have REE abundances more than 25× chondrite, exhibiting a more enriched E-MORB character. REE patterns for subalkaline dolerites are similar to those for the tholeiites, and vary from N- to E-MORB affinity. Most, however, correspond more closely to E-MORB (Fig. 13).

3.4. Age of the third generation dikes

Two samples (8324 and 8330) of fresh dolerites were chosen from the third generation dikes

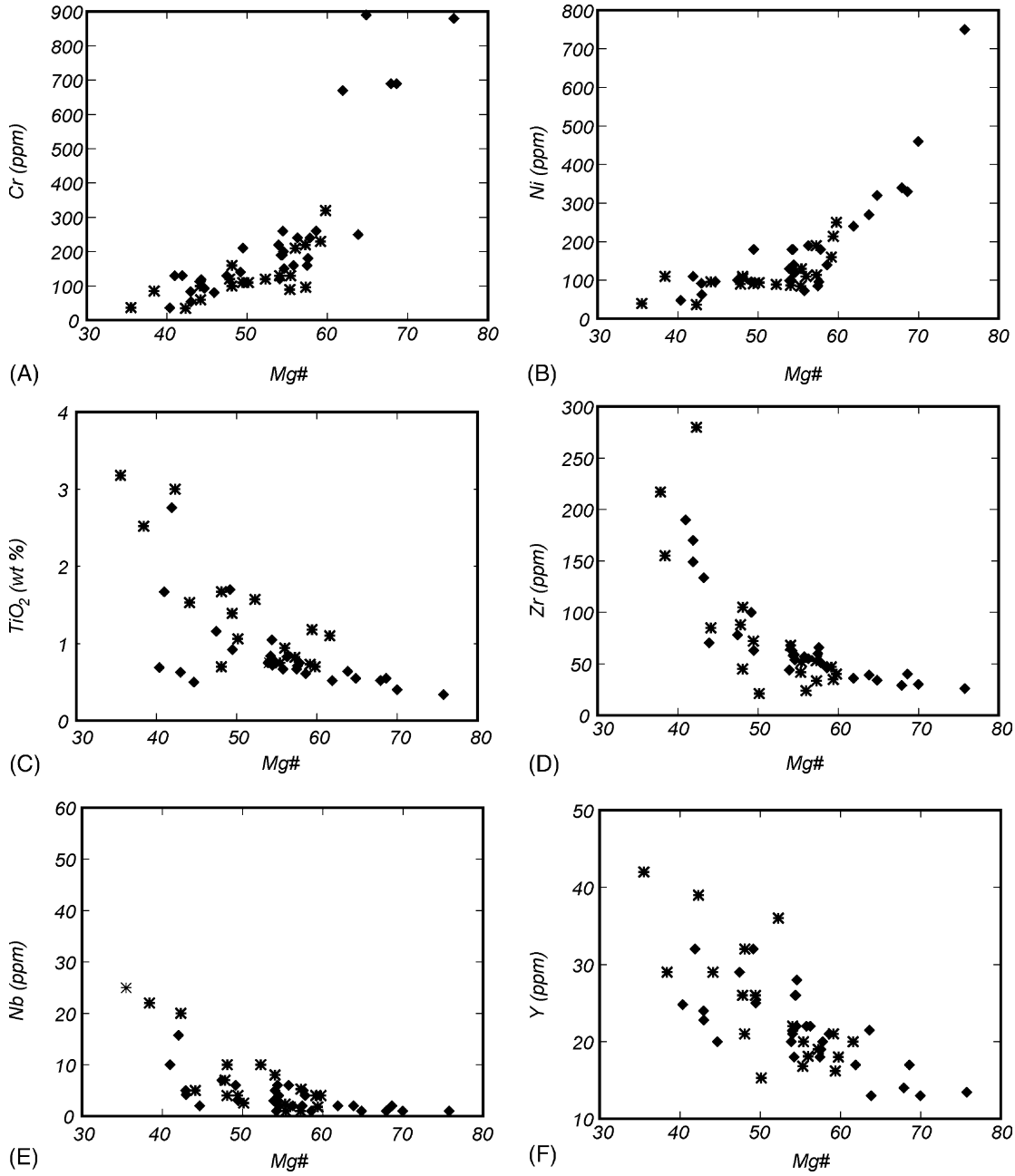

Fig. 9. Variations of (A) Cr; (B) Ni; (C) TiO_2; (D) Zr; (E) Nb; and (F) Y vs. magnesium number (Mg#). Symbols as in Fig. 7.

for $^{40}Ar/^{39}Ar$ (plagioclase) and Sm–Nd (mineral isochron) isotopic studies. Sample locations are shown in Fig. 6, and whole rock analyses are presented in Table 2. These samples were little affected by secondary alteration, and have medium grain size for easy mineral separation. Mineral separates were obtained from samples by standard magnetic and heavy liquid methods followed by hand picking. Only

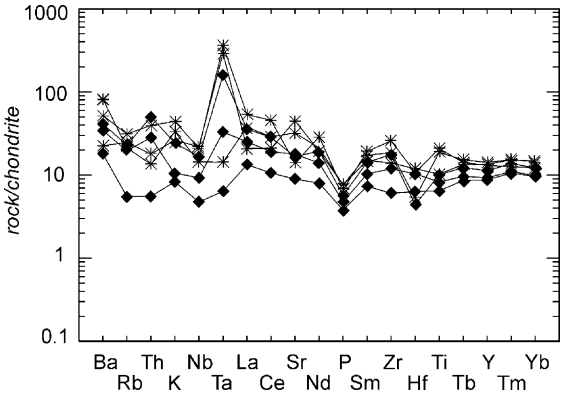

Fig. 10. Chondrite-normalised abundances of trace elements in dolerites. Normalising values after Sun and McDonough (1989), except for Rb, K, and P, which are from Sun (1980). Symbols as in Fig. 7.

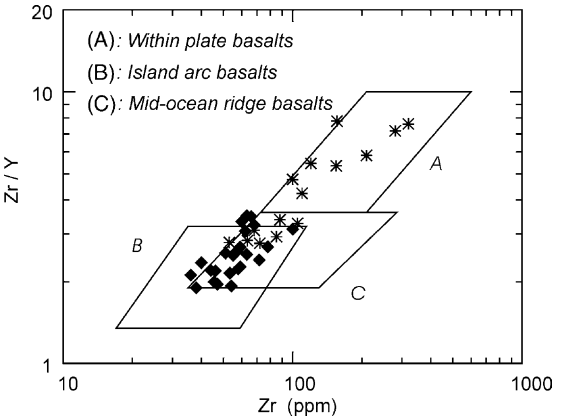

Fig. 12. Zr/Y–Zr tectonic discrimination diagram (Pearce and Norry, 1979) for third generation dolerites. Symbols as in Fig. 7.

transparent grains of plagioclase were selected to avoid the effects of secondary alteration.

$^{40}Ar/^{39}Ar$ analyses were carried out in the United Institute of Geology, Geophysics and Mineralogy (Siberian Branch of the Russian Academy of Science, Novosibirsk). The MSA-11 standard, calibrated on Hd-Bio and LP-6-Bio international standards, was used. Calculation of $^{40}Ar/^{39}Ar$ ages was made using the criteria proposed by Fleash et al. (1977). Only the experiment with sample 8330 yielded a relatively well-defined mean plateau age of 758 ± 4 Ma (57.9% of the cumulative ^{39}Ar gas) (Table 3, Fig. 14). The primary plagioclase in sample 8324 was significantly altered by low-temperature processes. The saddle form of the spectrum (Fig. 14) is indicative of excess radiogenic argon (Lanphere and Dalrymple, 1976), so this age should be interpreted with caution.

Sm–Nd analysis was carried out on a Finnegan MAT 262 mass spectrometer at the Graduate School, Division of Earth and Planetary Science, Hokkaido University. Sample preparation and analytical techniques are given by Kagami et al. (1989), Orihashi et al. (1998), and Agashev et al. (2001). The $^{143}Nd/^{144}Nd$ ratio for plagioclase was checked by additional measurements at Niigata University (by Dr.

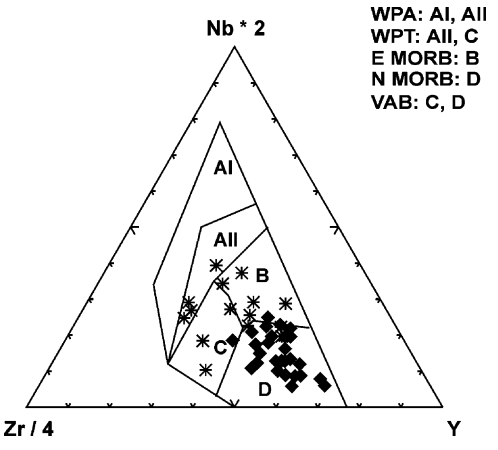

Fig. 11. Nb–Zr–Y tectonic discriminant diagram of Meschede (1986) for dolerites. Symbols as in Fig. 7. WPA: within-plate alkaline basalts; WPT: within-plate tholeiite; E-MORB: enriched mid-ocean ridge basalt; N-MORB: normal mid-ocean ridge basalt; VAB: volcanic arc basalt.

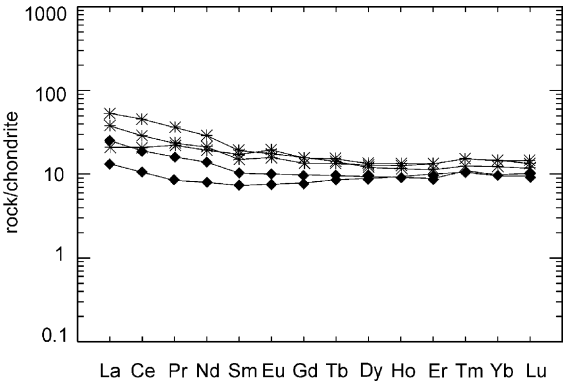

Fig. 13. Chondrite-normalised (Sun and McDonough, 1989) REE patterns for dolerites. Symbols as in Fig. 7.

Table 3
Results of $^{40}Ar/^{39}Ar$ dating of the gabbro-dolerites from the Sharyzhalgai massif (sample 8330)

Step	Age (Ma)	$^{40}Ar/^{39}Ar$	$^{38}Ar/^{39}Ar$	$^{37}Ar/^{39}Ar$	$^{36}Ar/^{39}Ar$	Cumulative ^{39}Ar (%)
1	787.2 ± 17.8	500.2 ± 8.1	0.268 ± 0.0418	18.9 ± 0.4	0.926 ± 0.0211	3.1
2	806.9 ± 7.4	283.5 ± 2.6	0.079 ± 0.0059	35.0 ± 0.3	0.168 ± 0.0035	15.4
3	689.2 ± 7.4	218.9 ± 2.1	0.037 ± 0.0018	36.1 ± 0.3	0.088 ± 0.0046	34.4
4	767.8 ± 5.0	238.0 ± 1.5	0.034 ± 0.0010	15.7 ± 0.1	0.062 ± 0.0012	61.0
5	946.7 ± 11.2	351.3 ± 4.3	0.076 ± 0.0070	13.6 ± 0.2	0.221 ± 0.0064	69.1
6	936.5 ± 6.5	351.5 ± 2.6	0.136 ± 0.0016	13.9 ± 0.1	0.235 ± 0.0025	100.0

$J = 0.002413 \pm 0.00001$.

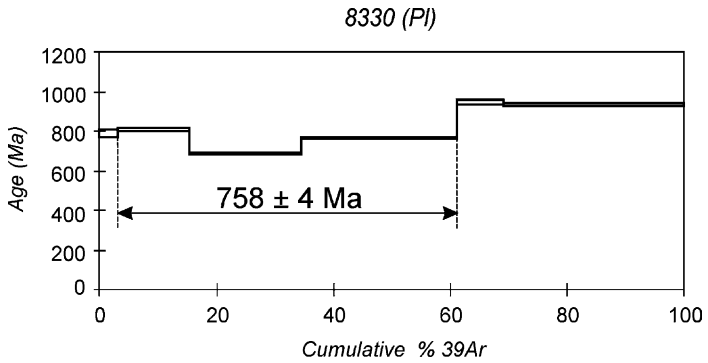

Fig. 14. Age spectrum for plagioclase (sample 8330) from Neoproterozoic dolerites of the Sharyzhalgai metamorphic massif.

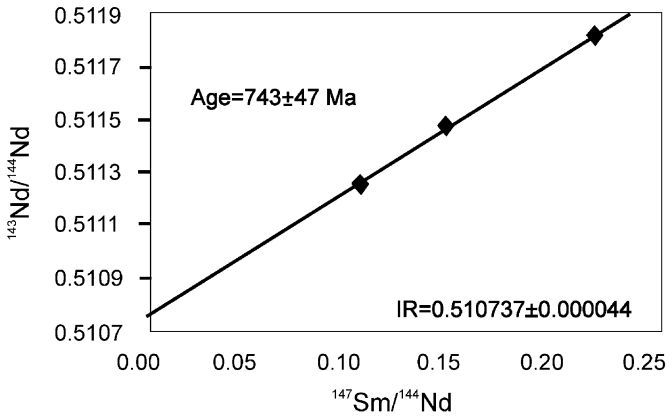

Sample	$^{147}Sm/^{144}Nd$	$^{143}Nd/^{144}Nd$	2σ	Sm (ppm)	Nd (ppm)
8330 WR	0.150	0.511477	0.000008	0.954	3.84
8330 Cpx	0.223	0.511816	0.000012	0.823	2.23
8330 Pl	0.108	0.511260	0.000036	0.069	0.39
JNdi-1 (2001/5/4, Niigata Univ.)		0.512065	0.000013		
JNdi-1 (Tanaka et al., 2000)		0.512119	(La Jolla is 0.511858)		

Fig. 15. Sm–Nd whole rock-mineral isochron diagram and isotope data for dolerite of the Sharyzhalgai metamorphic massif (sample 8330). WR: whole rock, Cpx: clinopyroxene, Pl: plagioclase.

Ikawa), but no significant difference was detected. The Pl-Cpx-WR-isochron for sample 8330 yields an age of 743 ± 47 Ma (Fig. 15), with an initial $^{143}Nd/^{144}Nd$ ratio of 0.510737 ± 0.000044. The relatively large error on the calculated age is a result of the very low Sm content of plagioclase, but nonetheless, the age is in broad agreement with the $^{39}Ar/^{40}Ar$ age from the same sample.

4. Discussion

Among the different dike generations distinguished in the Sharyzhalgai metamorphic massif, only non-metamorphosed third generation dolerite dikes are abundant and important for reconstruction of the Meso- to Neoproterozoic evolution of the Siberian craton. Metamorphosed dikes of the first and second generations are relatively scarce, and are inferred to be contemporaneous with, or older than, the time of the last high-temperature metamorphism at ca. 1860 Ma (Aftalion et al., 1991).

Dolerite dikes of the third generation are abundant all over the Sharyzhalgai metamorphic massif. In some areas they form relatively narrow swarms with a predominant NNW-SSE orientation. This orientation is oblique to the NW-SE trending craton boundary (see Fig. 1B), raising the question of whether or not they were related to the break-up of a supercontinent. However, this obliquity could reflect Phanerozoic tectonic modification of this craton boundary (e.g. Zonenshain et al., 1990).

Geochemical features of the third generation dolerite dikes suggest that there was a single magmatic source for both the tholeiitic and subalkaline varieties. On binary diagrams (Fig. 9) all values fall in a single trend, implying that all the third generation dikes were probably intruded during a single magmatic episode.

Ti/Yb ratios in the tholeiites and subalkaline dolerites are moderate, from 1130 to 4133, with an overall mean of 2343. Such values indicate that although some crustal contamination took place, it was not significant (Hart et al., 1989). La/Nb ratios of >1.5 in the tholeiitic and subalkaline dolerites suggest derivation from slightly enriched lithospheric sources (Fitton et al., 1988). Both tholeiitic and subalkaline dolerites have high La/Ta ratios (average 41). Thompson and Morrison (1988) suggested that ratios >30 are typical of melts derived from lithospheric sources. These authors also noted that high La/Nb and La/Ta ratios, typical of subcontinental lithosphere, are normally connected to the enrichment of lithospheric mantle by subduction-related melts and fluids produced during previous tectonic events. However, McDonough (1990) demonstrated that subcontinental lithosphere is not everywhere infiltrated by subduction fluids, which led him to suggest that the subcontinental lithosphere was heterogeneous, consisting of depleted and relatively enriched parts. Negative Nb anomalies (Fig. 10) are visible in both the tholeiites and subalkaline dolerites. Such anomalies may be caused by involvement of a subduction-modified mantle source. The enrichment of the mantle source by subduction components might be related to the Paleoproterozoic subduction processes along the southern margin of the Siberian craton. Relics of Paleoproterozoic ophiolite and eclogite complexes (Sklyarov et al., 1998; Gladkotchub et al., 2000) in the Sharyzhalgai massif are indicative of the operation of the subduction processes. Positive Ta anomaly in trace-elements patterns (Fig. 10) and Th/Ta ratio of <1 may suggest a plume origin for the initial melts. Thus, trace elements patterns and ratios suggest that both tholeiitic and subalkaline basalts may have been derived from a single lithospheric source enriched by Paleoproterozoic subduction and mantle plume activities.

Isotopic dating indicates that the third generation dikes are of Neoproterozoic age. The $^{40}Ar/^{39}Ar$ plateau age of 758 ± 4 Ma (sample 8330, 57.9% of the cumulative ^{39}Ar gas) is compatible with the Sm–Nd isochron age of 743 ± 47 Ma. However, further isotopic investigations are still needed.

There is a general acceptance for the likely existence of a supercontinent Rodinia, formed by collisional events in the late Mesoproterozoic and early Neoproterozoic (McMenamin and McMenamin, 1990). The position of Siberia in Rodinia is disputed (Hoffman, 1991; Condie and Rosen, 1994; Sears and Price, 1978, 2000; Frost et al., 1998; Rainbird et al., 1998; Pisarevsky et al., 2003), but it is generally shown as lying along either the northern or the western margin of Laurentia (present coordinates). Positions of Precambrian dike swarms may help to test these and other reconstructions.

There are two giant radiating dike swarms in northern Laurentia—the 1269–1265 Ma Mackenzie

swarm and the 727–721 Ma Franklin swarm (Ernst et al., 1996). If Siberia and Laurentia were parts of a single continent in the Meso- and/or Neoproterozoic, as it shown on the reconstructions of Hoffman (1991), Condie and Rosen (1994), Frost et al. (1998), and Rainbird et al. (1998), the traces of these enormous magmatic events might be expected to occur in Siberia. The reconstructions of Frost et al. (1998) and Rainbird et al. (1998) are of particular interest for our study because both of them place the southern margin of Siberia adjacent to the northern margin of Laurentia (present coordinates). On the other hand, an extensive ~780 Ma mafic magmatic event, probably related to the rifting event is well known in western Laurentia (Ross et al., 1995; Ernst et al., 1996).

Our study did not reveal any evidence for Mackenzie-age magmatism, but the new Sm–Nd date of 743 ± 47 Ma for the third generation dikes is roughly comparable with both the Franklin event in northern Laurentia and/or the ~780 Ma event in western Laurentia. Furthermore, the geochemical study supports the suggestion that most of the third generation dikes in the Sharyzhalgai massif (and possibly also in adjacent areas) could have been intruded during one large magmatic event. It is possible that it was an event in the middle of a large Laurentia-Siberia continent. However, we realise that more geochronological and geochemical data are required to test this hypothesis. In addition, dikes of the Nersinsk complex cut the sediments of the Karagas Group (which has an inferred age of 1100–900 Ma) in different parts of the Pre-Sayan area. The Sharyzhalgai third generation dikes belong to the Nersinsk complex, and the Karagas Group is usually interpreted as a passive margin succession (e.g. Sklyarov et al., 2001 and references therein). This implies that the passive margin already existed along the southwestern boundary of Siberia before the intrusion of these dikes. This suggests the presence of an oceanic basin along the southern boundary of the Siberian craton in Meso- to Neoproterozoic time and thus contradicts the reconstructions of Frost et al. (1998) and Rainbird et al. (1998). The suggestion of a ca. 1200–700 Ma "Poseidon" ocean to the north (present coordinates) of Laurentia (Frisch and Trettin, 1991 and references therein) does not support these reconstructions either.

5. Conclusions

Precambrian dikes of the Sharyzhalgai massif were intruded during at least three separate magmatic events. The oldest dikes are pre-late Paleoproterozoic. They were strongly deformed and metamorphosed during a high *P–T* event probably between 2000 and 1900 Ma. Dikes of the second generation were intruded during a low-*P* high-*T* metamorphic event, probably caused by the extensional collapse of the Paleoproterozoic orogen at 1890–1860 Ma. They are less abundant than both younger and older dikes. Dikes of the third generation are non-metamorphosed and largely unaltered. Geochemical study of these dikes shows that they include both tholeiitic and subalkaline types that were probably intruded during a single magmatic event. New 743 ± 47 Ma Sm–Nd and 758 ± 4 Ma $^{40}Ar/^{39}Ar$ plateau ages suggests that this generation of dikes could be correlated with the 727–721 Ma Franklin magmatic event, or with the ~780 Ma western Laurentian event in the middle of a large Laurentia-Siberia continent. However, more precise geochronological data are needed to confirm the age of the dike suite.

Acknowledgements

This study was supported by the Russian Fundamental Science Foundation (Grants 00-15-98576, 01-05-6400, 01-05-97237, 02-05-64481) and by the Science Support Foundation, Russia (grant for talented young researchers). We thank Nick Karmanov and Sergei Kanakin for their assistance with the mineralogical investigations. T. Watanabe would like to express his thanks to Professor Maruyama of the Tokyo Institute of Technology for financial support. The manuscript benefited immensely from the formal reviews of R. Weinberg and R. Ernst and informal reviews by T. Rivers and B.P. Roser. This is Tectonics Special Research Centre publication #192, and a contribution to International Geological Correlation Program (IGCP) Project 440.

References

Aftalion, M., Bibikova, E.V., Bowes, D.R., Hopwood, A.M., Perchuk, L.L., 1991. Timing of early Proterozoic collisional and

extensional events in the granulite-gneiss–charnockite–granite complex, Lake Baikal, USSR: a U–Pb, Rb–Sr and Sm–Nd isotopic study. J. Geol. 99, 851–861.

Agashev, A.M., Watanabe, T., Kuligin, S.S., Pokhilenko, N.P., Orishasi, Y., 2001. Rb–Sr and Sm–Nd isotopes in garnet pyroxenite xenoliths from Siberian kimberlites: an insight into lithospheric mantle. J. Mineral. Petrol. Sci. 96, 7–18.

Bukharov, A.A., 1987. Ancient Activated Zones of Ancient Platforms. Novosibirsk, Nauka, 202 pp.

Condie, K.C., Rosen, O.M., 1994. Laurentia-Siberia connection revisited. Geology 22, 168–170.

Dalziel, I.W.D., 1997. Neoproterozoic-Paleozoic geography and tectonics: review, hypothesis, environmental speculation. Geol. Soc. Am. Bull. 109, 16–42.

Domyshev, V.G., 1976. Riphean Mafic Rocks of the Baikal–Sayan–Yenisey Marginal Part of the Siberian Platform. Novosibirsk, Nauka, 87 pp. (in Russian).

Droop, G.T.R., 1987. A general equation for estimating Fe^{3+} concentrations in ferromagnesian silicates and oxides from microprobe analyses, using stoichiometric criteria. Mineral. Mag. 51, 431–435.

Ernst, R.E., Buchan, K.L., Hamilton, M.A., Okrugin, A.V., Tomshin, M.D., 2000. Integrated paleomagnetism and U–Pb geochronology of mafic dikes of the eastern Anabar Shield region, Siberia: implications for Mesoproterozoic paleolatitude of Siberia and comparison with Laurentia. J. Geol. 108, 381–401.

Ernst, R.E., Buchan, K.L., West, T.D., Palmer, H.C., 1996. Diabase (dolerite) dyke swarms of the world: first edition. Geol. Surv. Can. Open File 3241.

Fitton, J.G., James, D., Kempton, P.D., Ormerod, D.S., Leeman, W.P., 1988. The role of lithospheric mantle in the generation of late Cenozoic basic magmas in the western United States. In: Cox, K.G., Menzies, M.A. (Eds.), Oceanic and Continental Lithosphere: Similarities and Differences. J. Petrol. Spec., vol. 331–349.

Fleash, R.J., Sutter, J.F., Elliot, D.H., 1977. Interpretation of discordant $^{39}Ar/^{40}Ar$ age-spectra of Mesozoic tholeiites of Antarctica. Geochim. Cosmochim. Acta 41, 15–32.

Frisch, T., Trettin, H.P., 1991. Precambrian successions in the northernmost part of the Canadian shield. In: Trettin, H.P. (Ed.), Geology of the Innuitian Orogen and Arctic Platform of Canada and Greenland. Geological Survey of Canada, Geology of Canada, no. 3, pp. 103–108 (Chapter 6).

Frost, B.R., Avchenko, O.V., Chamberlain, K.R., Frost, C.D., 1998. Evidence for extensive Proterozoic remobilization of the Aldan shield and implications for Proterozoic plate tectonic reconstructions of Siberia and Laurentia. Precamb. Res. 89, 1–23.

Garbe-Schonberg, C.-D., 1993. Simultaneous determination of thirty-seven trace elements in twenty-eight international rock standards by ICP-MS. Geostand. Newsl. 17, 81–97.

Gladkotchub, D.P., Sklyarov, E.V., Donskaya, T.V., Mazukabzov, A.M., Menshgin, Yu.V., Panteeva, S.V., 2001. Petrology of gabbro-dolerites from Neoproterozoic dike swarms of the Sharyzhalgai massif: contribution to the problem of Rodinia break-up. Petrology 9, 639–656.

Gladkotchub, D.P., Sklyarov, E.V., Menshagin, Yu.V., Mazukabzov, A.M., 2000. Geochemical affinities of ancient ophiolites of the Sharyzhalgai massif. Geochemistry 10, 1039–1051.

Hart, W.K., WoldeGabriel, G., Walter, R.C., Merzman, S.A., 1989. Basaltic volcanism in Ethiopia: constraints on continental rifting and mantle interactions. J. Geophys. Res. 94, 7731–7748.

Hoffman, P.F., 1991. Did the breakout of Laurentia turn Gondwana inside out? Science 252, 1409–1412.

Kagami, H., Yokose, H., Honma, H., 1989. $^{87}Sr/^{86}Sr$ and $^{143}Nd/^{144}Nd$ ratios of GSJ rocks reference samples. Geochem. J. 23, 209–214.

Khomentovsky, V.V., 1996. The event of the Neoproterozoic stratigraphic scale for Siberia and China. Russian Geol. Geophys. 37, 35–47 (in Russian).

Lanphere, M.A., Dalrymple, G.B., 1976. Identification of excess ^{40}Ar by the $^{40}Ar/^{39}Ar$ age spectrum technique. Earth Planet. Sci. Lett. 32, 141–148.

Le Bas, M.J., Le Maitre, R.W., Streckeisen, A., Zanettin, B., 1986. A chemical classification of volcanic rocks based on the total alkali-silica diagram. J. Petrol. 27, 745–750.

McDonough, W.F., 1990. Constraints on the composition of the lithospheric mantle. Earth Planet. Sci. Lett. 101, 1–18.

McMenamin, M.A.S., McMenamin, D.L.S., 1990. The Emergence of Animals: The Cambrian Breakthrough. Columbia University Press, New York, 217 pp.

Meschede, M., 1986. A method of discriminating between different types of mid-ocean ridge basalts and continental tholeiites with the Nb–Zr–Y diagram. Chem. Geol. 56, 207–218.

Neimark, L.A., Larin, A.M., Nemchin, A.A., Ovchinnikova, G.V., Rytsk, E.Y., 1998. Geochemical, geochronologic (U–Pb) and isotopic (Pb, Nd) evidence of the anorogenic nature of magmatism in the north-Baikal volcanic-plutonic belt. Petrology 6, 139–164 (in Russian).

Orihashi, Y., Maeda, J., Tanaka, R., Zeniya, R., Niida, K., 1998. Sr and Nd isotope data for the seven GSJ rock reference samples JA-1, JB-2, JB-3, JG-1a, Lgb-1, and JR-1. Geochem. J. 32, 205–211.

Park, J.K., Buchan, K.L., Harlan, S.S., 1995. A proposed giant radiating dike swarm fragmented by the separation of Laurentia and Australia based on paleomagnetism of ca. 780 Ma mafic intrusions in western North America. Earth Planet. Sci. Lett. 132, 129–139.

Pearce, J.A., Norry, M.J., 1979. Petrogenetic implications of Ti, Zr, Y and Nb variations in volcanic rocks. Contrib. Mineral. Petrol. 69, 33–47.

Pisarevsky, S.A., Wingate, M.T.D., Powell, C.McA., Johnson, S., Evans, D.A.D., 2003. Models of Rodinia assembly and fragmentation. In: Yoshida, M., Windley, B.F. (Eds.), Proterozoic East Gondwana: Supercontinent Assembly and Break-up. Geol. Soc. London Spec. Publ. 206, in press.

Plaksenko, A.N., 1989. Typomorphism of the Accessory Chromespinels from Ultramafic Magmatic Complexes. VGU Press, Voronezh, 222 pp. (in Russian).

Rainbird, R.H., Stern, R.A., Khudoley, A.K., Kropachev, A.P., Heaman, L.M., Sukhorukov, V.I., 1998. U–Pb geochronology of Riphean sandstone and gabbro from southeast Siberia and

its bearing on the Laurentia-Siberia connection. Earth Planet. Sci. Lett. 164, 409–420.

Ross, G.M., Bloch, J.D., Krouse, H.R., 1995. Neoproterozoic strata of the southern Canadian Cordillera and the isotopic evolution of seawater sulfate. Precamb. Res. 73, 71–99.

Sears, J.W., Price, R.A., 1978. The Siberian connection: a case for Precambrian separation of the North American and Siberian cratons. Geology 6, 267–270.

Sears, J.W., Price, R.A., 2000. New look at the Siberian connection: no SWEAT. Geology 28, 423–426.

Sekerin, A.P., Yu, V., Laschenov, V.A., 1991. Riphean mafic series of the Urik-Tumanshet zone of the Pri-Sayan area. Soviet Geol. 2, 58–64 (in Russian).

Sekerin, A.P., Menshgin, Yu.V., Laschenov, V.A., 1995. Pre-Sayan province of high-K alkaline mafic rocks and lamproites. Dokl. RAN 342, 82–86 (in Russian).

Sklyarov, E.V., Gladkochub, D.P., Mazukabzov, A.M., Stankevich, M.A., Donskaya, T.V., Konstantinov, K.M., Sinzov, A.V., 2001. Indicator Complexes of Supercontinent Rodinia Break-up. Geological Excursion Guide of Workshop Supercontinents and Geological Evolution of Precambrian. Institute of Earth Crust, Irkutsk, 75 pp. (in Russian).

Sklyarov, E.V., Gladkochub, D.P., Mazukabzov, A.M., Menshagin, Yu.V., Konstantinov, K.M., 2000. Dike swarms of southern margin of the Siberian craton- indicators of Rodinia supercontinent break-up. Geotectonics 6, 59–75.

Sklyarov, E.V., Gladkochub, D.P., Mazukabzov, A.M., Menshagin, Yu.V., 1998. Metamorphism of ancient ophiolites of the Sharyzhalgai block (Siberia, Russia). Russian Geol. Geophys. 39, 1722–1739.

Sryvtsev, N.A., 1986. The structure and geochronology of the Akitkan series of the western Baikal area. In: Ryazanov, Z.V. (Ed.), Problems of Stratigraphy of Precambrian of Siberia. Moscow, Nauka, pp. 50–61 (in Russian).

Sun, S.S., 1980. Lead isotopic study of young volcanic rocks from mid-ocean ridges, ocean islands and island arcs. Phil. Trans. R. Soc. 297, 409–445.

Sun, S., McDonough, W.F., 1989. Chemical and isotopic systematics of oceanic basalts: implications for mantle composition and processes. In: Saunders, A.D., Norry, M.J. (Eds.), Magmatism in the Oceanic Basins, Geol. Soc. London. Spec. Pub. 42, 313–345.

Thompson, R.N., Morrison, M.A., 1988. Asthenospheric and lower-lithospheric mantle contributions to continental extension magmatism: an example from the British Tertiary Province. Chem. Geol. 68, 1–15.

Winchester, J.A., Floyd, P.A., 1976. Geochemical magma type discrimination: application to altered and metamorphosed igneous rocks. Earth Planet. Sci. Lett. 28, 459–469.

Zonenshain, L.P., Kuzmin, M.I., Natapov, L.M., 1990. Geology of the USSR: A Plate-Tectonic Synthesis. Geodynamics Series, 21, AGU, Washingtoton, DC, 242 p.